

## Surface Roughness Scaling of Plasma Polymer Films

G. W. Collins, S. A. Letts, E. M. Fearon, R. L. McEachern, and T. P. Bernat

*Lawrence Livermore National Laboratory, Livermore, California 94551*

(Received 10 January 1994)

Atomic force microscopy data reveal self-affine scaling of plasma polymer films. The rms surface roughness  $\sigma$  increases with film thickness  $\tau$  as  $\sigma(f < \xi^{-1}) \sim \tau^\beta$ , and with measurement length  $L$  as  $\sigma(f > L^{-1} > \xi^{-1}) \sim L^\alpha$ , where  $\xi$  is the surface roughness correlation length. At the deposition rate  $R = 2 \mu\text{m/h}$ , the scaling exponents  $\alpha$  and  $\beta$  are 0.9 and 0.7, both increasing to 1 at  $R = 1 \mu\text{m/h}$ . A competition between surface relaxation and deposition rate determine  $\sigma$  and  $\xi$ , which increase rapidly with  $R$  or inverse temperature.

PACS numbers: 68.55.Bd, 05.70.Ln, 68.55.Jk

Comparison between self-affine surface structure data, computer simulations, and theoretical models is often made using scaling exponents for the rms surface roughness  $\sigma(L, t)$  [1–3]:

$$\sigma(L, t) = \left[ \langle h(\mathbf{r}, t)^2 \rangle_r - \langle h(\mathbf{r}, t) \rangle_r^2 \right]^{1/2} \sim \begin{cases} t^\beta, & t < cL^\alpha, \\ L^\alpha, & t \gg cL^\alpha, \end{cases} \quad (1)$$

where  $t$  is the time,  $\mathbf{r}$  is the position in the plane perpendicular to the growing direction,  $h(\mathbf{r}, t)$  is the height of the surface at time  $t$  and position  $\mathbf{r}$ ,  $\langle h(\mathbf{r}, t) \rangle_r$  is the spatial average of  $h(\mathbf{r}, t)$ ,  $L$  is the length of the surface measured, and  $c$  is a constant. Thus,  $\sigma$  initially scales with time as  $t^\beta$  but shows a saturated scaling as  $L^\alpha$  for thick layers [4]. Knowing the functional form of  $\alpha$  and  $\beta$  in terms of process conditions allows the prediction of the surface roughness for any sample size.

For simple random deposition with no spatial or temporal correlations between the deposited particles (the extreme kinetic limit),  $\beta = 0.5$ , since  $\sigma$  grows as a “random walk,” and  $\alpha = 0$ , since there is no saturated scaling with  $L$ . For a real surface, relaxation processes such as in the Langevin type models couple the 2 degrees of freedom in the surface roughness,  $L$  and  $t$ , so as to change the scaling exponents. For example, Edwards and Wilkinson (EW) [5] use a Langevin equation [Eq. (2) with  $\lambda = 0$ ] to model the evolution of a surface, and find in  $d = 1 + 1$  dimensions  $\alpha = \frac{1}{2}$  and  $\beta = \frac{1}{4}$ . In  $d = 2 + 1$  the power law behavior in Eq. (1) changes to a logarithmic dependence. Kardar, Parisi, and Zhang (KPZ) [6] allowed for a component of interface growth parallel to the plane. They used the equation

$$\frac{dh(\mathbf{r}, t)}{dt} = \nu \nabla^2 h(\mathbf{r}, t) + \frac{\lambda}{2} [\nabla h(\mathbf{r}, t)]^2 + \eta(\mathbf{r}, t), \quad (2)$$

where  $\nu$  is related to surface relaxation,  $\eta$  is the random fluctuation in the incoming flux, which is assumed to be Gaussian with delta function correlation  $\langle \eta(\mathbf{r}, t) \eta(\mathbf{r}', t') \rangle = 2D \delta(\mathbf{r} - \mathbf{r}', t - t')$ , and  $\lambda$  is the growth velocity perpendicular to the surface. In  $d = 1 + 1$  dimensions they obtained the exponents  $\alpha = \frac{1}{2}$  and  $\beta = \frac{1}{3}$ . In  $d = 2 + 1$ , Amar and Family [7] find that when  $10 \leq \lambda^2 D / 2\nu^3 \leq 25$ ,  $\beta \sim 0.25$  and  $\alpha \sim 0.4$ , while for  $\lambda^2 D / 2\nu^3 \sim 1$ , the

effective value of  $\beta$  decreases. This connects the scaling exponent  $\beta$  to the surface relaxation process ( $\sim \nu$ ), and the deposition rate ( $\sim D$ ).

For the growth of plasma polymer films presented here we find  $1 > \alpha > 0.9$  and  $1 > \beta > 0.6$ . Of the experimental studies of the deposition of thin films, only a few have been analyzed in terms of both scaling laws of Eq. (1) [8]. For these studies  $1 \geq \alpha \geq 0.2$  and  $0.56 \geq \beta \geq 0.22$  [9]. The values of  $\alpha$  overlap our own, but our values of  $\beta$  are significantly larger, and are intuitively difficult. Theoretical work [2–7,10] involving various relaxation mechanisms for surface fluctuations predict values of  $\alpha$  that, depending on the model, span our observed range, but find values of  $\beta$  reduced from the “random deposition” value of 0.5. However, Amar and Family obtain  $\beta = 1$  in three dimensions from numerical solutions to a continuum equation in which the dominant relaxation process is diffusion along the surface [11]. Also, models including surface pinning [12] and shadowing can produce  $\beta > 0.5$ . The “extreme kinetic limit” model including shadowing produces  $\beta \sim 1$  for isotropic coating, and  $\beta \sim 0.3$  when the maximum deposition angle  $\phi$  is not greater than  $80^\circ$  from the growing direction [13]. A similar shadowing model with  $\phi < 70^\circ$ , that allows surface relaxation predicts  $\beta \sim 0.7$  in the high temperature limit [14]. Although we cannot definitively say what characteristic distinguishes plasma polymer films from other experiments, the high pressures used in this deposition process may induce shadow instabilities leading to larger  $\beta$ 's [13,14].

Most of our experiments are at constant substrate temperature ( $T = 318 \text{ K}$ ) but varying deposition rate  $R$ . For one set of deposition parameters, yielding  $R = 2 \mu\text{m/h}$ , we find  $\alpha \sim 0.9$  and  $\beta \sim 0.7$ . For  $R > 0.9 \mu\text{m/h}$ ,  $\alpha$  and  $\beta$  decrease slightly with increasing  $R$  and both  $\sigma$  and the transverse correlation length increase rapidly with  $R$ . At  $R \sim 1 \mu\text{m/h}$ , we have investigated the substrate temperature dependence of  $\sigma$ . It is relatively temperature independent until  $T > 353 \text{ K}$ , where  $\sigma \sim \exp(\text{const}/T)$ . We suggest the dependence of  $\sigma$  on  $R$  and  $T$  is due to a competition between the surface relaxation rate and the deposition rate.

The coatings were prepared in an inductively coupled rf driven plasma discharge [15]. The system and the plasma coating process have been previously described [16,17]. Briefly, the system consists of a supply manifold with controlled gas flow rates, an rf discharge generator, a coating chamber, and a vacuum pump. The reactant gases were trans-2-butene (T2B) and hydrogen. We measure and control the pressure in the coating chamber. The polymer deposition occurs in a region of glow discharge. The reactive fragments produced in the discharge chemically recombine in the gas phase and on nearby surfaces to form the amorphous polymer coating. The films were deposited on a cleaned silicon wafer substrate at 318 K. The atomic composition of these polymer films is determined by combustion microchemical analysis to be  $\text{CH}_{1.3}$  and the chemical structure is thought to resemble a highly crosslinked polyethylene.

The plasma polymer surfaces were characterized with atomic force microscopy (AFM) using a Digital Instruments Nanoscope III with a commercial silicon nitride tip of radius  $\sim 30$  nm. The cantilever spring constant was 0.12 N/m giving a contact force of 120 nN. The scan rate was between 0.9 and 2 Hz. We analyzed data from three different scan sizes:  $40 \mu\text{m} \times 40 \mu\text{m}$ ,  $10 \mu\text{m} \times 10 \mu\text{m}$ , and  $2 \mu\text{m} \times 2 \mu\text{m}$  each with 512 lines of 512 points per line.  $\sigma$  is calculated by the AFM software, and is the standard deviation of height values in a given two-dimensional section.

We also calculate the averaged power spectrum from the spectra of each of the 512 linear traces. Thus, in contrast to  $\sigma$ , the power spectra are calculated from one-dimensional cross sections of the surface. Each spectrum is the square of the surface roughness amplitude per spatial frequency interval and the integral over all frequencies is the mean-square surface roughness within the measured bandwidth ( $\sigma^2$ ). For plotting the spectra shown here, we multiply the power,  $P(f)$ , by the length of the AFM measurement so as to scale the roughness per frequency the same for different size measurements.

Figure 1 is  $P(f)$  for a 10 and 40  $\mu\text{m}$  measurement of the same plasma polymer surface. This film was formed on a 318 K substrate with  $R = 1.4 \mu\text{m/h}$ , resulting from a total pressure of 72 mtorr, and  $\text{H}_2$  flow rate,  $F_{\text{H}_2} = 11.6$  SCCM ( $\text{cm}^3/\text{min}$  at STP), and a T2B flow rate,  $F_{\text{T2B}} = 0.226$  SCCM. The total film thickness was 27  $\mu\text{m}$ . The power spectra in Fig. 1 has two distinct regions. The flat, low frequency part resembles uncorrelated white noise. The sloped portion extending over two decades of spatial frequency represents the correlated portion of the surface roughness. This power law region of the power spectra depends on  $R$  and  $T$ . To obtain the scaling exponent  $\alpha$  from this data we fit the power law decay to

$$P(f > \xi^{-1}) = \frac{\text{const}}{f^\gamma} \quad (3)$$

and for  $\gamma \geq d'$  [18]

$$\alpha = \frac{(\gamma - d')}{2}, \quad (4)$$

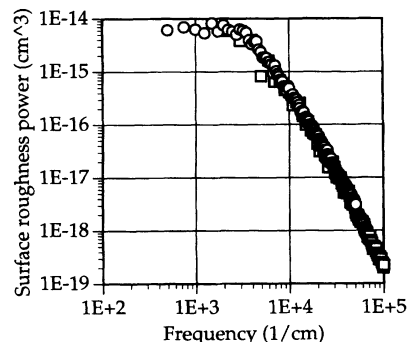


FIG. 1. Surface roughness power spectra for 10  $\mu\text{m}$  (squares) and 40  $\mu\text{m}$  (circles) measurements of a 27  $\mu\text{m}$  thick plasma polymer film shows power law behavior over several decades.

where  $d'$  is the dimension of the cross section through the data, which in this case equals 1. To characterize the scale of correlations perpendicular to the growing direction, we define the correlation frequency  $\xi^{-1}$  as the spatial frequency where  $P(f)$  has fallen to  $1/e$  of its low frequency value and above which  $\sigma$  is correlated. For Fig. 1 we find  $\gamma = 3$ ,  $\alpha = 1$ ,  $\xi^{-1} = 5750 \text{ cm}^{-1}$ . Although the values of  $\gamma$  and  $\alpha$  vary slightly with the deposition conditions, the general shape of the power spectrum remains the same.

Figure 2(a) shows power spectra of 10  $\mu\text{m}$  AFM patches from surfaces grown under the same deposition conditions but to different thicknesses.  $R$  was 2  $\mu\text{m/h}$  which resulted from  $F_{\text{T2B}} = 0.38$  SCCM,  $F_{\text{H}_2} = 11.6$  SCCM, and a total pressure of 72 mTorr. The substrate was at 318 K. In general the high frequency components do not increase with increasing thickness, but the low frequency components do. We fit Eq. (3) to the high frequency part of  $P(f)$  for the three thickest films to obtain  $\gamma = 2.8$ . Using Eq. (4) we determine  $\alpha$  to be  $0.90 \pm 0.07$  [19]. The black squares in Fig. 2(b) show  $\sigma$  versus thickness for the surfaces represented in Fig. 2(a). To obtain  $\beta$ , we fit our data to  $\sigma = (\text{const})\tau^\beta$ , which is the analog to the top line in Eq. (1), where  $\tau$  is the thickness of the film [20]. This data is not saturated with  $\tau$  and we find  $\beta = 0.7$ . Thus the self-affine scaling relations, Eq. (1) and Eq. (3), describe our data for lengths  $100 \text{ nm} < L < 40 \mu\text{m}$  and thicknesses,  $10 \text{ nm} < \tau < 100 \mu\text{m}$ . The black squares in Fig. 2(c) show  $\xi$  versus  $\tau$  for the power spectra of Fig. 2(a). This should scale as  $\xi \sim \tau^{\beta/\alpha}$ , and fit to the data gives  $\beta/\alpha = 0.7$ , close to the value predicted.

Figures 2(b) and 2(c) also show  $\sigma$  and  $\xi$  for surfaces with different  $R$ 's. For a large range of deposition parameters,  $R$  increases with increasing  $F_{\text{T2B}}$ , or decreasing  $F_{\text{H}_2}$ . For data in this paper we kept  $F_{\text{H}_2} = 11.6$  SCCM and varied  $F_{\text{T2B}}$  where we find  $R(\mu\text{m/h}) = 4.9F_{\text{T2B}}(\text{SCCM}) + 0.28$ . We determine  $\gamma$  from the power spectra decay,  $\beta/\alpha$  from  $\xi(\tau)$ , and  $\beta$  from  $\sigma(\tau)$ . For  $R = 2 \mu\text{m/h}$ ,  $\gamma = 2.8$ ,  $\beta/\alpha = 0.7$ , and  $\beta = 0.7$ . For  $R = 1.48 \mu\text{m/h}$ ,  $\gamma = 2.9$ ,  $\beta/\alpha = 0.9$ , and  $\beta = 0.9$ . For  $R = 1 \mu\text{m/h}$ ,  $\gamma = 3.2$ ,  $\beta/\alpha = 1$ , and  $\beta = 1.0$ . At  $R = 0.8 \mu\text{m/h}$  the

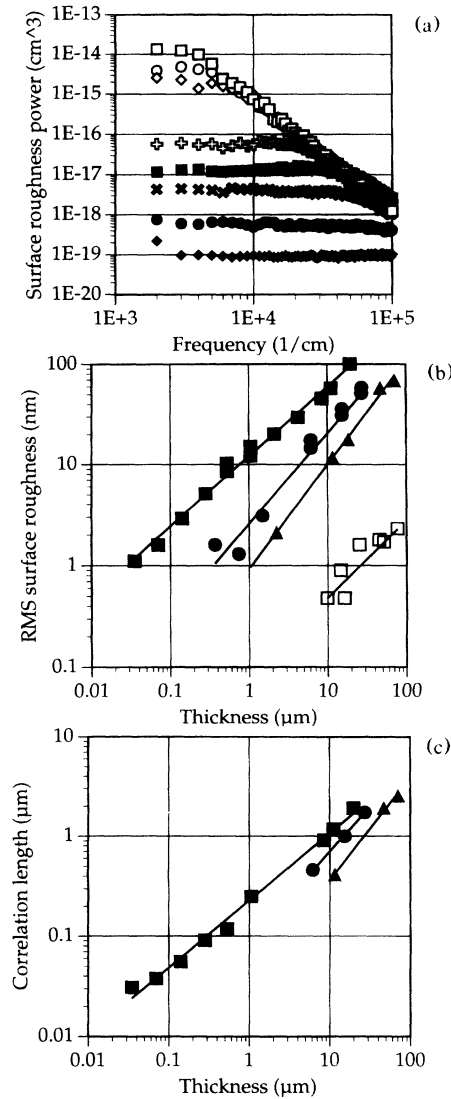


FIG. 2. (a) Evolution of the surface roughness power spectra with increasing film thickness: 19.7 μm (open squares), 11.1 μm (open circles), 8.5 μm (open diamonds), 1.1 μm (crosses), 0.53 μm (dark squares), 0.28 μm (×), 0.14 μm (dark circles), and 0.07 μm (dark diamonds). (b) RMS surface roughness versus thickness for films grown with deposition rates 2 μm/h (black squares), 1.5 μm/h (black circles), 1 μm/h (black triangles), and 0.8 μm/h (open squares). (c) Transverse correlation length versus thickness for films grown with deposition rates 2 μm/h (black squares), 1.5 μm/h (black circles), and 1 μm/h (black triangles). The lines going through the data are from the fits discussed in the text.

data was too smooth to reliably determine  $\gamma$  or  $\alpha$ , but we find  $\beta \sim 0.7$ . The error bars are  $\pm 0.2$  for  $\gamma$ ,  $\pm 0.1$  for  $\beta/\alpha$ , and  $\pm 0.1$  for  $\beta$ . Thus we do not see a statistically significant variation in  $\alpha$ , but we do find significant variations in  $\beta$  versus deposition rate. Furthermore, films grown with  $R < 0.9 \mu\text{m/h}$  are smoother, with a  $\beta$  lower than anticipated by extrapolating  $\beta$  from the three data sets with higher  $R$ 's.

In Fig. 3, we combine several measurements of the  $\sigma$  versus  $R$  by removing the thickness dependence. As the ratio  $F_{T2B}/F_{H_2}$  increases the films become more stressed [16] and we show here that the surfaces are also rougher. Figure 3 shows  $\sigma/\tau^\beta$  versus  $R$ . The data follow a power law

$$\sigma/\tau^\beta = 0.415R^{4.46}. \quad (5)$$

We have also fit  $\xi/\tau^{\beta/\alpha}$  (taking  $\alpha = 1$ ) versus  $R$  and obtain

$$\xi/\tau^{\beta/\alpha} = 0.0319R^{2.6}. \quad (6)$$

Thus, the scale of correlations perpendicular ( $\xi$ ) and parallel ( $\sigma$ ) to the growing direction both increase rapidly with  $R$ . Also, surface perturbations grow in height faster than in width with increasing  $R$  [21].

Figure 4 shows the temperature dependence of  $\sigma$  and  $\xi$  after removing the  $\tau$  and  $R$  dependence,  $\sigma/(0.415R^{4.46}\tau^\beta)$  and  $\xi/(0.0319R^{2.6}\tau^{\beta/\alpha})$ . We assume here that  $\beta$  and  $\alpha$  are roughly independent of temperature compared to  $\sigma$  and  $\xi$ . The precursor gas flow rates were  $F_{T2B} = 0.28$  SCCM and  $F_{H_2} = 5.2$  SCCM.  $R$  varied linearly with decreasing temperature as  $R(\mu\text{m/h}) = 5 - 0.01T$ , where  $T$  is in kelvin. We see that  $\sigma$  is roughly independent of temperature below 353 K and then decreases exponentially with increasing temperature as  $\sigma/(0.415R^{4.46}\tau^\beta) \sim \exp(13200/T)$ .  $\xi$  also decreases with increasing temperature, but not as rapidly as  $\sigma$ . Note that this is the same trend that we saw between  $\sigma$  and  $\xi$  when the  $R$  was varied [Eqs. (5) and (6)] at constant temperature. The power spectra also show an increase in all frequency components with decreasing temperature. This is different than the evolution of the power spectra with thickness at constant rate where only the low frequency components increase with increasing thickness. Thus, at higher temperatures, the increased surface relaxation rate allows the short wavelength roughness amplitudes to relax towards longer wavelengths faster, giving rise to a smoother surface.

The sharp decrease in  $\sigma$  versus  $R$  at constant  $T$  and  $\sigma$  versus  $T$  at roughly constant  $R$ , implies a competition between surface relaxation and deposition rate. At a low temperature and large deposition rate, particles at the

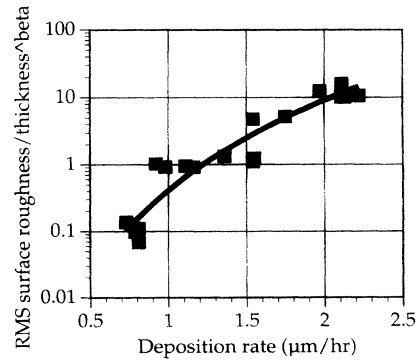


FIG. 3. Rate dependence of the RMS surface roughness with the thickness dependence removed,  $\sigma/\tau^\beta$ , where  $\sigma$  is in nanometers, and  $\tau$  is in microns. The line going through the data is from the fit discussed in the text.

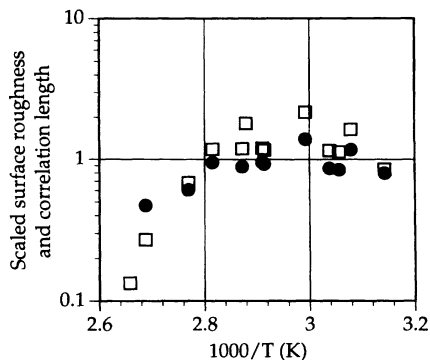


FIG. 4. Temperature dependence of the RMS surface roughness (open squares) and transverse correlation length (black circles) both with the thickness and rate dependence removed. The scaled RMS surface roughness is  $\sigma/(\tau^\beta 0.415R^{4.46})$ , the scaled correlation length is  $\xi^{-1}/(\tau^{\beta/\alpha} 0.0319R^{2.6})$ , where  $\sigma$  is in nanometers,  $\tau$  and  $\xi$  are in microns, and  $R$  is in microns per hour.

surface cannot relax quickly enough before the next layer of material is deposited. Similarly, at high temperature the relaxation rate is increased to the point where a low deposition rate is too slow to be relevant in the microscopic relaxation process.

In summary, most experimental and theoretical efforts describing surface growth have focused on deposition processes similar to molecular beam epitaxy or sputtering, and yield scaling exponents,  $0.2 \leq \alpha \leq 1$ , and  $0.2 \leq \beta \leq 0.56$  [4–10]. We report the first observation of dynamic scaling from a plasma induced chemical vapor deposition process. We find the scaling exponents,  $0.9 \leq \alpha \leq 1$  and  $0.6 \leq \beta \leq 1$ , depending on the deposition rate. Although we cannot definitively say what characteristic distinguishes plasma polymer films from experiments with  $\beta < 0.6$ , the high pressures used in this deposition process may induce shadow instabilities, increasing  $\beta$  [13,14]. In Eqs. (5) and (6) we report the first observation of the scaling behavior of either the RMS surface roughness or the correlation length on the deposition rate. At a constant deposition rate and “low temperature,” both the RMS surface roughness and the correlation length are temperature independent. At higher temperature we find a crossover temperature, ( $T \sim 353$  K at the deposition rate of  $1 \mu\text{m/h}$ ), above which the RMS surface roughness and the correlation length decrease rapidly with increasing temperature.

This work was performed under the auspices of the U.S. Department of Energy by the Lawrence Livermore National Laboratory under Contract No. W-7405-ENG-48.

- [1] T. Vicsek, *Fractal Growth Phenomena 2nd Ed.* (World Scientific, Singapore, 1992).
- [2] F. Family and T. Vicsek, *Dynamics of Fractal Surfaces* (World Scientific, Singapore, 1991).
- [3] P. Meakin, *Phys. Rep.* **235**, 189 (1993).
- [4] F. Family and Tamas Vicsek, *J. Phys. A* **18**, L75 (1985).
- [5] S. F. Edwards and D. R. Wilkinson, *Proc. R. Soc. London A* **381**, 17 (1982).

- [6] M. Kardar, G. Parisi, and Y. C. Zhang, *Phys. Rev. Lett.* **56**, 889 (1986).
- [7] J. G. Amar and F. Family, *Phys. Rev. A* **41**, 3399 (1990).
- [8] Y. L. He, H. N. Yang, T. M. Lu, and B. C. Wang, *Phys. Rev. Lett.* **69**, 3770 (1992); H. You, R. P. Chiarello, H. K. Kim, and K. G. Vandervoort, *Phys. Rev. Lett.* **70**, 2900 (1993); H. J. Earnst, F. Fabre, R. Forkerts, and J. Lapujoulade, *Phys. Rev. Lett.* **72**, 112 (1994).
- [9] Other work has measured either  $\alpha$  or  $\beta$ , whose values also lie in the stated ranges. For example, P. Herrasti, P. Ocon, P. Vazquez, R. C. Salvarezza, J. M. Vara, and A. J. Arvia, *Phys. Rev. A* **45**, 7440 (1992); R. C. Salvarezza, L. Vazquez, P. Herrasti, P. Ocon, J. M. Vara, and A. J. Arvia, *Europhys. Lett.* **20**, 727 (1992); J. Chevrier, V. Le Thanh, R. Buys, and J. Derrien, *Europhys. Lett.* **16**, 737 (1991); P. Pfeifer, Y. J. Wu, M. W. Cole, and J. Krim, *Phys. Rev. Lett.* **62**, 1997 (1989).
- [10] For example, J. Villian, *J. Phys. I (France)* **1**, 19 (1991); D. E. Wolf and J. Villian, *Europhys. Lett.* **14**, 389 (1990); M. Kotrla, A. C. Levi, and P. Smilauer, *Europhys. Lett.* **20**, 25 (1992); M. Siegert and M. Plischke, *Phys. Rev. Lett.* **68**, 2035 (1992); S. Das Sarma and S. V. Ghaisas, *Phys. Rev. Lett.* **69**, 3762 (1992); J. Krug, M. Plischke, and M. Siefert, *Phys. Rev. Lett.* **70**, 3271 (1993); L.-H. Tang and T. Nattermann, *Phys. Rev. Lett.* **66**, 2899 (1991); D. A. Kessler, H. Levine, and L. M. Sander, *Phys. Rev. Lett.* **69**, 100 (1992); Z. W. Lai and S. Das Sarma, *Phys. Rev. Lett.* **66**, 2348 (1991).
- [11] J. G. Amar and F. Family, “Continuum Model of Epitaxial Roughening” (unpublished). In several previous works including surface diffusion,  $\beta < 0.5$ . For example, Kessler, Levin, and Sander in Ref. [10], and H. Yan, *Phys. Rev. Lett.* **68**, 3048 (1992). Amar and Family do not discuss the reason for the difference in  $\beta$ 's compared to similar previous work, although a crossover regime at early times (or thin coverages) between this result and KPZ scaling is found.
- [12] M. H. Jensen and I. Procaccia, *J. Phys. II (France)* **1**, 1139 (1991).
- [13] C. Tang and S. Liang, *Phys. Rev. Lett.* **71**, 2769 (1993).
- [14] C. Roland and H. Guo, *Phys. Rev. Lett.* **66**, 2104 (1991). These results for  $\beta$  are qualitatively similar to those found by Earnst *et al.* in Ref. [8].
- [15] H. Yasuda, *Plasma Polymerization* (Academic, New York, 1985).
- [16] S. A. Letts, D. E. Miller, R. A. Corley, T. M. Tillotson, and L. A. Witt, *J. Vac. Sci. Technol. A* **3**, 1277 (1985).
- [17] S. A. Letts, D. W. Myers, and L. A. Witt, *J. Vac. Sci. Technol.* **19**, 739 (1981).
- [18] R. F. Voss, in *Scaling Phenomena in Disordered Systems*, edited by R. Pynn and A. Skejeltorp (Plenum, New York, 1985), p. 1–11.
- [19] The thinner films shown in Fig. 2(a) yielded a slightly lower power law exponent ( $\sim 2.6$ ), but the fewer data points yielded a much lower confidence in these data.
- [20] For our constant flux process, the film thickness is proportional to time, and this equation yields the same result for  $\beta$  as Eq. (1).
- [21] The fit for  $\sigma/\tau^\beta$  included data at  $0.8 \mu\text{m/h}$  while there was no correlation length data at that rate. When the  $0.8 \mu\text{m/h}$  data is ignored we obtain  $\sigma/\tau^\beta = 0.68R^{3.7}$ , still a larger exponent for the rate dependence than  $\xi^{-1}/\tau^{\beta/\alpha}$ .